N74-16237

Paper No. 5

THERMAL TESTING OF THE VIKING LANDER IN SIMULATED MARTIAN ENVIRONMENTS

T. Buna and T. R. Tracey, *Martin Marietta Aerospace, Denver Div., Denver, Colorado*
T. W. E. Hankinson, *NASA Langley Research Center, Hampton, Virginia*

ABSTRACT

Techniques for the simulation of the Martian Thermal Environment are Verified by Full Scale Test Data

INTRODUCTION

The presence of a dynamic atmosphere on Mars introduces a probabilistic element into the definition of the mission environment of a Martian lander. This precludes the possibility of "mission thermal simulation" in a test facility, in the usual sense applicable to spacecraft testing. The available alternative is to bracket the multitude of possible thermal conditions at the landing site with simulated "hot" and "cold" extremes which guarantee the survival of the lander under all anticipated conditions on Mars. This paper reviews the definitions of thermal test extremes applicable to the Viking Lander, and discusses the criteria, techniques and facilities required for their simulation in light of recent data obtained from Mars Simulation tests conducted with the Viking Thermal Effects Test Model (TETM).

The TETM is a full scale model of the Viking Lander, incorporating the developmental thermal control subsystem, flight type structures, and thermal simulators of science and electronic equipment. The primary objective of the Mars simulation tests was to verify the lander thermal design and supporting analytical models, and to demonstrate the adequacy of the test techniques. The discussion in this paper is limited to the latter aspects of the test results; the thermal response of the vehicle being only considered to the extent necessary to demonstrate the test approach. The relation of the TETM Mars simulation test program to the other Viking thermal tests is illustrated on Figure 1.

In the above context, the TETM tests represent the final link in a chain of developmental efforts initiated early during the Viking program and aimed at the definition of a suitable Mars simulation test approach. These developments included the definition of the test environments and facility requirements (1,2)[1], implementation of the necessary facility modifications,

[1]The numbers in parenthesis refer to the list of references appended to this paper.

and investigations related to unique test-operational features of Mars environmental simulation (3,4). The final proof of the proposed technique, however, was dependent on the availability of a full scale thermal model of the Lander, since the simulation techniques are related to convective processes which depend in detail on vehicle-peculiar forcing geometries and heat dissipation profiles. These vehicle-induced convective effects in the test environment impose limitations on both the controllability of the test environment, and the ability to separate the performance of the test facility from that of the test article.

In addition to the precursory developmental effort already mentioned, of particular significance are the "RTG Wind Tunnel Tests" depicted on the left hand side of Figure 1. Their purpose was to provide data for the design of protective wind shields for the RTG's, and to determine the effects of winds on the availability of RTG waste heat for thermal control. The results of the wind tunnel tests served as input in the form of controlled ETG boundary conditions during the TETM cold extreme test.

In the next section, the definition of the simulated thermal extremes is reviewed, and criteria for their simulation are developed. This is followed by descriptions of the simulation approach, the test hardware, and test operations. A discussion of test results as spplied to the simulation technique is presented in the last section.

NOMENCLATURE

f	=	parameter defined by Equation (2)
h	=	convective coefficient, Btu/hr-ft^2-^{o}R
h^*	=	equivalent convective coefficient defined by Equation (7e), Btu/hr-ft^2-^{o}F
P	=	period of Martian diurnal cycle - 24.66hours (= 1480 min., approx.)
q	=	heat flux per unit area of skin, Btu/hr-ft^2
t	=	time from Martian midnight, hr
T	=	temperature, ^{o}R
$\bar{T}$	=	average temperature for the Martian diurnal cycle, ^{o}R
ΔT_R	=	difference between radiation-equilibrium and skin temperature, ^{o}R = $T_{R,M} - T_s$
ϵ	=	vehicle outer surface emissivity
σ	=	Stefan-Boltzmann constant, Btu/hr-ft^2-^{o}F

Subscripts

abs	=	radiation absorbed from the environment (sum of IR, solar and albedo)
em	=	radiation emitted by vehicle outer surface
CH	=	simulation chamber
h	=	convection
min	=	minimum (lower extreme)

max = maximum (upper extreme)
M = Mars
R = radiation-equilibrium (as attained in the absence of convection)
s = outer surface of the vehicle (vehicle/environment thermal interface)
∞ = Martian atmosphere

SIMULATION CRITERIA

In order to arrive at a definition of the simulated extremes, consider the heat balance of the vehicle outer skin in the non-dimensional form derived in Reference 1:

$$(T_{s,M}/T_{R,M})^4 + f(T_{s,M}/T_{R,M}) - f(T_{s,M}/T_{\infty}) - 1 = 0 \qquad (1)$$

where:
$$f = h_M/\epsilon\sigma T_{R,M}^3 \qquad (2)$$

$$T_R = \left(\frac{q_{tr,M} + q_{abs,M}}{\epsilon\sigma}\right)^{1/4} \qquad (3)$$

The above equations may be applied to either local/instantaneous values of the temperatures and heat transfer coefficients, or to averages over time and/or surface areas. In the latter case the averaging should be in accordance with the various components of heat fluxes, hence fourth-power averages apply to the first term in Equation (1), whereas algebraic averaging pertains to the linear terms.

Equation (1) is plotted with f as a parameter on Figure 2, an examination of which indicates the following. For a given vehicle surface, all possible thermal conditions are bracketed by the two intersecting straight lines $f = 0$ and $f = \infty$, and the point of intersection divides the environments into two regimes designated as "convective cooling" and "convective heating" regimes, respectively. In the convective cooling regime, maximum vehicle temperatures are attained in the absence of winds (convection minimized) approaching T_R in the limit. The opposite applies to the convective heating regime.

In the most general case, the various elements of a lander may operate in different thermal regimes at a given time, or may cross over (through the point of intersection at which $T_R = T_{\infty} = T_s$) from one regime to the other during a given period of time.

For given operational modes of the lander, mission span, and landing site, extreme values for both T_{∞} and T_R may be established as functions of diurnal cycle, independently from the convective environments on Mars. The extremes of T_{∞} are defined by the Mars Environmental Models depicted on Figure 5 of Reference 5. The extremes of T_R may be calculated from Equation (3) with good approximation, since neither q_{tr} nor q_{abs} are significantly dependent on wind effects. For the general case where the surface "crosses over" from one thermal regime to the other during the diurnal period, these profiles may look as shown on Figure 3, an examination of which indicates the following.

522-137 O - 73 - 5

The theoretical upper limit for the vehicle surface temperature is given by the curve ABCDE. In order for the vehicle surface to approach this limit, it would be necessary that radiation dominated conditions (zero wind) prevail from A through B, and D through E, whereas maximum wind conditions dominate from B through D. This implies a step function increase in wind velocity from zero to maximum at B, and a corresponding decrease at D. This is a highly improbable condition, especially considering the fact, that it would have to repeat itself during two consecutive Martian days, to produce significant thermal effects on the equipment compartment. On the other hand, a "probable" upper limit of the temperatures will be represented by the curve ABFDE on Figure 3, provided that

$$\overline{T}_{R,M,max} = \frac{1}{P}\int_0^P T_{R,M,max}\,dt \gg \frac{1}{P}\int_0^P T_{oo,max}\,dt$$

$$= \overline{T}oo,max \qquad (4)$$

Similar reasoning establishes the theoretical lower limit of the vehicle temperatures as the curve **abfde**, and the practical lower limit as **abcde**, on Figure 3, provided that:

$$\overline{T}_{oo,min} = \frac{1}{P}\int_0^P T_{oo,min}\,dt \ll \frac{1}{P}\int_0^P T_{R,M,min}\,dt =$$

$$\overline{T}_{R,M,min} \qquad (5)$$

As applied to the thermally significant vehicle/environment interfaces, the success criteria for the latter approach may be summarized as follows:

(1) The inequalities (4 and 5) must be satisfied,
(2) The radiation component of the "hot-extreme" environment must be accurately simulated,
(3) The temperature differences $(T_R - T_{s,CH}) \equiv \Delta T_R$ are within a pre-determined upper limit ($\Delta T_{R,max}$), established from estimates of minimum natural convective cooling on Mars, i.e.,

$$(T_{R,M} - T_{s,CH}) \leq \Delta T_{R,max} \qquad (6)$$

In the above inequality, $\Delta T_{R_{max}} = 10^{o}F$ (based on estimates of natural convection on Mars), $T_{s,CH}$ is supplied by the test data and $T_{R,M}$ is calculated by the use of Equation (3). Note that, with good radiation-simulation,

$$T_{R,CH} \approx T_{R,M}$$

within the approximation permitted by the compensating features to be discussed under Simulation Approach.

(4) The cold extreme simulation shall satisfy the requirement:

$$T_{s,CH} \trianglelefteq T_{s,M,min} \tag{7}$$

$T_{s,M,min}$ in Equation (7) may be deduced from the test data as follows:

$$h_M = \frac{q_{h,M}}{T_{s,M} - T_{oo}} \quad \text{(by definition)} \tag{7a}$$

and $$q_{h,M} = (q_{tr} + q_{abs} - q_{em})_M \quad \text{(from heat balance)} \tag{7b}$$

Furthermore, $$(q_{tr})_M = (q_{tr,CH}) \tag{7c}$$

and in view of (7) $$(q_{em})_M \trianglerighteq (q_{em})_{CH} \tag{7d}$$

By combining (7a through 7d) we have:

$$h^* \equiv \frac{q_{tr,CH} + q_{abs,M} - q_{em,M}}{T_{s,CH} - T_{oo,min}} \trianglerighteq h_{M,max} \tag{7e}$$

which is the explicit form of criterion (4) above.

An $h_{M,max} = 1$ was established for these tests from standard forced-convection correlations, as applied to maximum-wind conditions on Mars.

There are two general approaches that can be used to verify compliance with the above criteria for a given test. The first consists of comparing pre-test analytical predictions of $T_{s,M}$ profiles, with the corresponding $T_{s,CH}$ profiles supplied by the test data. This method has the advantage of possible attention to detail characteristic to large analytical models, however, it cannot separate the effects of convection and radiation in the chamber, and lacks the capability of independent verification of the test approach from that of the analytical model.

The second approach concentrates on the vehicle/environment interfaces only, and consists in determining the degree of approach of the $T_{s,CH}$ profiles to the $T_{R,M}$ and $T_{oo,M}$ profiles, as appropriate, per the discussions above. With this method, directly measured values of $q_{tr,CH}$ are all that is required to characterize the internal heat transfer processes of the lander, and the only calculated inputs (viz. q_{em} and q_{abs}), are connected with radiation processes. The convective effects in the chamber can be determined by solving the heat balance equation as applied to the vehicle skin. During the TETM tests, the $q_{tr,CH}$ were measured by commercial heat transfer gauges, and the results presented at the end of this paper are based on those measurements.

In addition to considerations of probability as noted above, a major factor entering into the definition of thermal extremes is the feasibility of techniques, and the availability of facilities, for their simulation. Clearly, an accurate simulation of thermal conditions implied by the curves ABCDE or abfde requires a test

facility combining the principal features of solar simulators, thermal vacuum chambers, and high-altitude wind tunnels, with special equipment required for atmospheric temperature control and for the simulatiom of the thermal properties of the Martian ground. Such a facility is presently outside the realm of practicality. On the other hand, the radiation-dominated domain represented by ABFDE and the convection domain represented by abcde on Figure 3 can be reproduced with acceptable accuracies, with specially equipped conventional thermal vacuum chambers, as discussed in the next section.

SIMULATION APPROACH

The TETM Mars surface simulation tests were conducted in Martin Marietta's Space Simulation Laboratory in Denver, Colorado, which has recently been equipped with planetary environmental simulation capabilities. The chamber adapted to Mars surface environmental simulation is schematically shown on Figure 4, on which the representative ranges of chamber environmental parameters are also indicated. The solar, planetary, and atmospheric ("sky") radiation components on Mars are reproduced in the facility by a 16-ft. dia. off-axis solar simulator, temperature-controlled ground thermal simulator, and a temperature-controlled shroud, respectively. The ground plane and the test article are mounted on a two-axis gimbal to provide rotation with respect to the solar vector for zenith and azimuth angle simulation (one-axis rotation only was used during the TETM tests). The chamber was "pressurized" with CO_2 to 2 torr during hot-extreme simulation, and with Argon to 35 torr during the cold-extreme tests. Argon was selected in lieu of CO_2 during the cold tests in order to prevent condensation on the cold shroud.

The conditions for the various test runs are summarized in Table 1. The objective of the cold soak runs was to provide steady-state heat transfer data for the purpose of verifying the conductor network in the thermal-analytical models and to evaluate thermal switch performance. They were preceeded by a "calibration run" conducted in vacuum with the purpose of verifying the external radiation conductor networks at various simulated zenith angles. Martian diurnal cycle simulation was accomplished during Runs 227, 223 and the second half of Run 231, and these will be the subject of further discussion. Unfortunately, Run 223 was not entirely successful because of partial overheating of the ground simulator, however, the data presented here pertain to areas of the lander not reflecting this anomaly.

Because of the dissimilarities inherent in the finite size of the thermal-vacuum chamber as opposed to the "open" environment on Mars, the following corrective or compensating features have been incorporated into the test approach:

(1) Compensation for finite ground simulator size by increased ground simulator temperatures,

(2) Substitution of IR radiation from the ground simulator for albedo on Mars, resulting in additional (although small) increase in required ground simulator temperatures,

(3) The simulation of dust cover on the lander surfaces, which could result in up to 70 percent increase in their solar absorptivity (with emissivity unchanged) by a 70 percent increase in solar constant in the simulated environment (Run 223).

(4) Compensation for excessive convective cooling during the hot extreme simulation tests by increased radiation levels in the chamber (as noted above). The higher convective levels are due in part to the higher gravitational constant on Earth, and in part to the colder sink temperatures provided by the shroud (which simulates "sky" temperatures) as compared to the atmospheric temperatures on Mars.

(5) Compensation for the absence of winds in the chamber during cold extreme simulation by the following:

  (a) Increased chamber pressure to 35 torr, as opposed to 15.2 torr max. on Mars to enhance natural convection.

  (b) Reduced chamber heat sink (shroud) temperatures 50 to 100 degrees F below the corresponding levels of $T_{oo,min}$, in order to enhance natural convective and radiation cooling.

  (c) Reduced thermal output from the RTG simulators to account for the decrease in the availability of RTG waste heat for thermal control during cold extreme conditions.

  (d) Reduced radiation levels in the chamber.

The ground simulator is a 22-ft diameter disc, covered with 19 individually controlled heater blankets, comprising a central disc, and two concentric rings surrounding the disc. Item (1) above was accomplished by increasing the emissive power of the outer ring by approximately 20 percent above Martian levels.

Items (2) and (3) resulted in increased temperatures of the inner ring as well, however, no further increase in the radiation levels was necessary to account for Item (4).

The upper limit in chamber pressure during the cold extreme simulation was set at 35 torr (Item 5a) to avoid undesirable internal convection within the equipment compartment of the lander. To prevent condensation of the chamber atmosphere on the shroud in view of Item 5b, argon was used as a chamber atmosphere in lieu of CO_2 during these tests. This provided additional conservatism to the test results, since the conductivity of argon (and hence, of the fiberglas insulation in the lander) was somewhat higher than that of CO_2.

Item 5c was in conformance with the results of the RTG Wind Tunnel Tests referred to earlier. The reduced output was controlled to predetermined RTG fin root temperatures as determined by these tests. Item 5d consisted (in addition to the effects of

the reduced shroud temperatures) in running the cold extreme tests with the solar simulator off, and a thermally passive ground simulator, in a horizontal position.

TEST ARTICLE AND SUPPORT EQUIPMENT

The test article and support equipment comprised several major elements, including: the TETM; Electrical Test Support Equipment (TSE); Space Simulation Laboratory (SSL); Test Fixtures; Data Processing Software; Data Reduction Support, and Assembly, Handling and Support Equipment. The TETM and its subsystems, the TSE, and the Data Processing Software, will be described briefly.

The Thermal Effects Test Model was designed to duplicate the thermal response of the Viking Lander when exposed to the simulated mission environments. It comprised six principal subsystems, including: Thermal Control, Structures, Non-functional Flight Type Equipment, Electrical Subsystem, Thermal Simulators, and an Instrumentation Subsystem. The Thermal Control Subsystem consisted of developmental hardware including multilayer and fiberglas insulation, erosion-resistant external coatings, internal thermal control coatings and finishes, thermal standoffs, and thermal switches. Special attention was given to minimizing test-peculiar thermal effects, such as by isolation of electrical and instrumentation cable feedthroughs.

The Structural Subsystem consisted of flight-type structures, including lander body, equipment mounting plate, and brackets. The non-functional flight-type equipment included cable harness (for heat-leak evaluation), developmental propulsion lines and valves assembly, and mounting brackets. There was no propellant fluid flow or storage requirements associated with the TETM program. Additionally, there was included a prototype unit of the soil sampler boom, and developmental landing legs.

The electrical subsystem comprised the heaters, cabling, and connectors for the thermal simulators of heat-dissipating equipment, including two Electrical Thermoelectric Generators (ETG's), which simulated the RTG's. Power control and monitoring of all electrical heaters within the TETM was accomplished by the TSE.

The function of the thermal simulators was to simulate the primary thermal characteristics of selected flight-type equipment, including: (a) the mounting thermal interfaces, by the use of flight-type mounting provisions; (b) the radiation/convection thermal interfaces, by preservation in the simulators of the geometry, size, and external optical properties of the flight equipment; (c) conduction coupling between the radiation and mounting interfaces, by preservation of the wall-conductances of equipment casings; (d) internal conduction paths; (e) total thermal mass; (f) total internal heat dissipation rate, with capabilities to approximate variable heat dissipation by step functions; (g) internal heat distribution (by the use of more than one heater element, when required), and (h) internal thermal mass distribution. The materials of construction for the simulators included

aluminum, steel, foam, and commercially available heater elements.

The TETM instrumentation consisted of temperature sensors, heat flow gauges, and strain gauges, the latter being included to comply with a secondary objective of the program to evaluate thermal strains within the structures. The vehicle-mounted thermal instrumentation comprised 648 measurements; 188 additional channels were used for monitoring electrical power to the TSE, ground simulator and shroud temperatures, solar intensities, and chamber pressures.

Typical simulator assemblies within the equipment compartment are shown on Figure 5, and the TETM during two consecutive stages of assembly is depicted on Figures 6 and 7, respectively. On Figure 7 the ETG's and the terminal propulsion tank simulators are exposed, the wind shields and the tank insulation being removed.

The function of the Electrical Test Support Equipment (TSE) was to supply, measure, and control electrical power to the thermal simulators and the ETG's. The power levels and distribution within the simulators were controlled by step functions representative of smoothed power profiles of the flight article. The power control was accomplished by the use of a pre-programmed drum switch, the switching from position to position being done manually according to a predetermined schedule.

The TETM Data Reduction Software was designed to provide quasi-real time data reduction and analysis.

The latter included calculations of heat balance, convective parameters, data averaging, data plotting, and predictions of times to stabilization.

TEST OPERATIONS

Preparatory to starting of the tests, a solar simulator calibration was performed, the chamber insulation was installed and several pumpdowns were performed in order to outgass and settle the insulation. The two-axis gimbal and the ground simulator, with the "closure panels" removed for access were installed in the chamber. An end-to-end power and instrumentation checkout was performed on the TETM outside the chamber.

Following the preparatory work, the TETM was installed into the chamber, and secured on the test adapter serving as the structural interface between the lander legs and the gimbal, and the gimbal and the ground simulator. Following the hookup of instrumentation and power cabling, the ground simulator closure panels were installed. This sequence of events is depicted on Figures 8, 9 and 10. The styro-foam insulation between the outer shell and the shroud of the chamber is shown on the lower part of Figure 8. The TETM is shown in the fully-assembled landed configuration, with the ETG's covered by wind shields, and the terminal propulsion tanks (partially covered by the wind shields) insulated.

The TETM was installed with the "science side" (the side closest to the technician on Figure 9) facing the simulated west on Mars, in order to provide worst-case orientation for the hot extreme tests.

Supplementing the quasi-real time monitoring provided by the TETM software, 100 pre-selected data channels were also monitored by the use of a real time data monitoring system which provided data printouts on command, and within five minutes of the actual data bursts.

Solar simulator on-off cycles, gimbal rotation, shroud temperature and ground simulator temperatures were controlled manually and were monitored with the RTM system.

The data were recorded on magnetic tapes by the "Astrodata" System, and the tapes removed on an average of 6-hour intervals for processing by the TETM software. Strict time-discipline was maintained in the data taking process, in order to provide accurate (Martian) day-to-day comparisons of temperatures for stability estimates. The same time-discipline was maintained with regard to all test support operations.

To assure the necessary flexibility for optimizing the simulation technique, in-test parameter modifications were permitted, and the test procedures redlined accordingly.

DISCUSSION OF TEST RESULTS

Typical temperature and heat flux profiles for test runs 227 and 231 are depicted on Figures 11 and 12, respectively. The curves indicate excellent repeatability of test conditions from one simulated Martian day to the other, and that periodic stability was essentially achieved within three Martian diurnal cycles. The heat flux profiles of Figures 11 and 12, represent traces from the same gauge, mounted on the side of the lander. The small fluctuations of heat flow within a Martian diurnal cycle are due to variations in the internal heat dissipation, and to shadowing effects from external components. The negative sign on the ordinate of these figures is in accordance with the convention assigning negative values to outgoing heat from the lander. A comparison of Figures 11 and 12 indicates that approximately twice as much heat was lost to the environment during the cold extreme tests, as compared to the hot extremes, the difference being supplied by the thermal switches from RTG waste heat.

Figures 13 through 17 are indicative of the quality of simulation achieved during the TETM tests. The vehicle skin temperatures closely approached (Martian) radiation equilibrium values during the hot extreme tests, with the temperature depression parameter ΔT_R always smaller than the specified limit of $10^{o}F$. It is also evident from the plots that the inequalities (4 and 5) were satisfied.

In order to determine the adequacy of radiation simulation during the hot extreme tests, $q_{abs,CH}$, averaged over the lander

sides, is compared with its corresponding Martian counter-part determined analytically, on Figure 13. The higher values of the chamber loads, expecially during the simulated Martian mid-day, served as "compensation" for excessive convective cooling in the chamber, and did not cause overheating, as evidenced by the temperature profiles applicable to the same locations on Figure 14.

Figure 15 indicates that inclusion of the lander top into the averaging of surface temperatures results in an increase of T_R and in operation within the convective cooling regime. This is due to increased solar absorption on the lander top, as compared to the sides, and to external heating from the RTG's. A similar effect is noted on Figure 16, which applies to the "dust covered lander", i.e. 170 percent solar constant. In this case the approach of $T_{s,CH}$ to $T_{R,M}$ is near-perfect.

Figure 17 shows typical temperature profiles during the cold-extreme simulation. Note that, on the average, the vehicle temperatures are considerably above Martian atmospheric temperatures, as implied by Equation (7e). The following values for h* have been determined by the use of Equation (7e) from the test data as averaged over the Martian diurnal cycle.

Lander sides, average: $h^* = 1.57$
Lander top, average: $h^* = 1.27$
Lander bottom, average: $h^* = 0.89$

The somewhat lower than "required" h* for the lander bottom is more than compensated for by the higher values on the sides and the top. It is further noted, that during the actual mission, atmospheric boundary layer effects will result in a decrease in wind speed and heat transfer coefficient near the ground.

CONCLUSIONS

1. The Viking lander thermal environments may be bracketed by a radiation-dominated hot extreme and a convection-dominated cold extreme. Both can be adequately simulated in modified conventional thermal vacuum facilities.
2. The hot extreme is completely defined by the radiation environment at the landing site and the heat dissipation requirements through the external surfaces of the lander. These may be resolved into a set of Radiation Equilibrium Temperature profiles, approached by the lander surfaces during "hot" operating conditions.
3. Due to its non-isotropic character, the Martian radiation environment must be accurately simulated during hot-extreme thermal testing.

4. The principal criterion for success for hot extreme simulation is the approach to radiation-equilibrium.

5. The effects of vehicle-induced convection inside the chamber during hot case simulation may be adequately compensated for by increased radiation levels.

6. The cold extreme is completely defined by the minimum atmospheric temperature profile at the landing site and an upper limit for the forced-convective coefficient, as applied to the lander.

7. The criterion of success for cold extreme simulation is that h* determined from heat losses in the chamber and the projected vehicle-environment temperature differences on Mars, shall equal or exceed the maximum forced convection coefficient on Mars.

8. Verification of the simulation approach during a test may be accomplished independently from the performance of the test article, provided the heat transferred through the vehicle skin is measured directly at predetermined locations. The correlation and consistency of the TETM data indicate that a limited number of judiciously located gauges suffice for this purpose.

9. The TETM Mars Simulation test program has demonstrated the feasibility and practicality of the test approach to be used on the qualification and flight articles.

REFERENCES

1. Buna, T., "Thermal Testing under Simulated Martian Environment", Progress in Astronautics and Aeronautics, Vol. 21, pp. 391-417, Academic Press, 1969.

2. VER-28, "Mars Surface Thermal Simulation", Martin Marietta Corporation, Denver Division, 27 January 1970.

3. Buna. T., and Ratliff, J.R., "Operation of a Large Thermal Vacuum Chamber at Martian Pressure Levels", National Bureau of Standards Special Publication 336, pp 725-748, October 1970

4. Buna, T., "Convective Heat Transfer in Simulated Martian Environments", Final Report, TOS T70-48888-001, Martin Marietta Corporation, Denver, Division, 1970.

5. Morey, T. F., and Tracey, T. R., "Mars Surface Thermal Environments for Viking Lander Design and Test", (In this volume).

TABLE 1 - TETM MARS SURFACE SIMULATION TEST PARAMETERS

TEST	COLD SOAK		HOT EXTREME		COLD EXTREME	
RUN NO.	201	202	223	227	231	
DESCRIPTION	ZERO POWER	MIN. POWER	"DUST" COVERED LANDER	NO DUST COVER	STEADY STATE ENV.	CYCLING ENV.
SOLAR BEAM, BTU/HR-FT^2	0		(170%) 346	(100%) 204	0	
ZENITH ANGLE	NA		CYCLING		NA	
GROUND SIM. TEMPERATURE	PASSIVE		CONTROLLED TEMP CYCLING		PASSIVE	
CHAMBER PRESS. & ATMOSPHERE	17.5 mbs CO2		2.7 mbs CO2		47 mbs ARGON	
SHROUD TEMP.	CONSTANT @ -180 F		CONSTANT @ -200 F		-240 F	CYCLING -240/-160F
ETG THERMAL OUTPUT	2 x 600 w		2 x 640 w		2 x 600 w	
INTERNAL POWER	0	MIN. AVG.	MAXIMUM DAILY DUTY CYCLE		MINIMUM DAILY DUTY CYCLE	

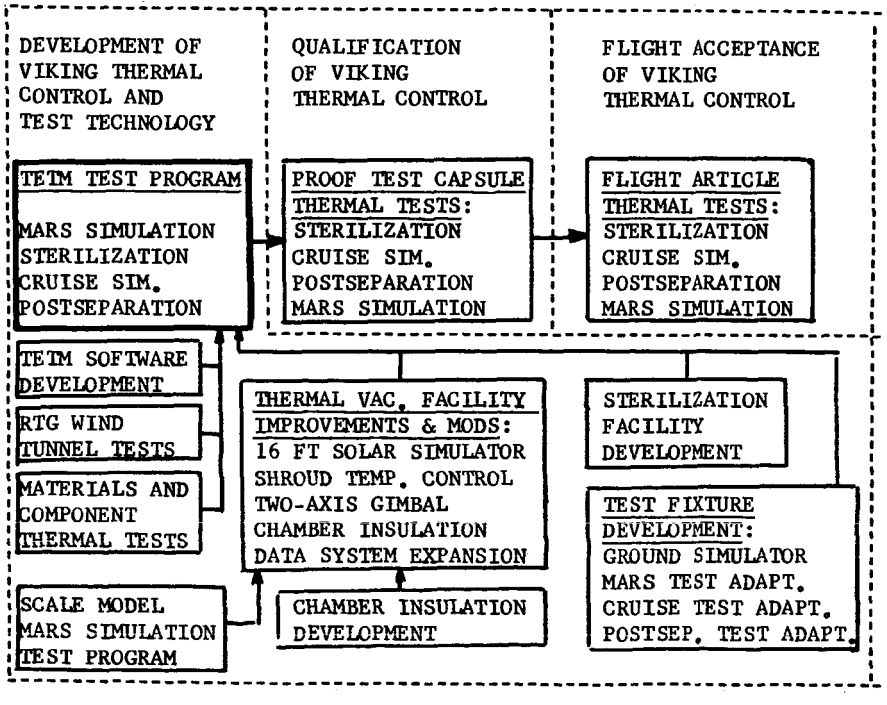

Fig. 1 — Relation of TETM other Viking thermal test programs

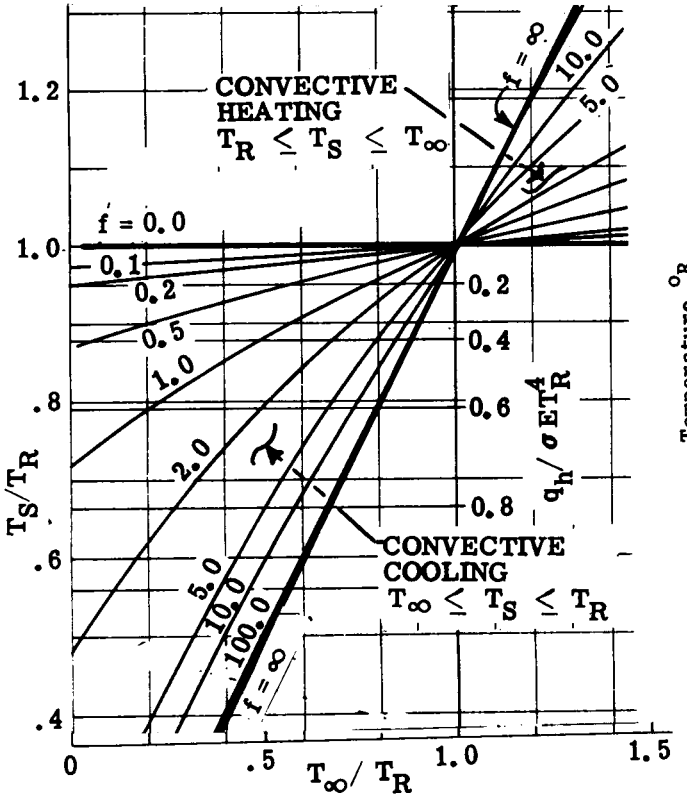

Fig. 2 – Definition of thermal regimes

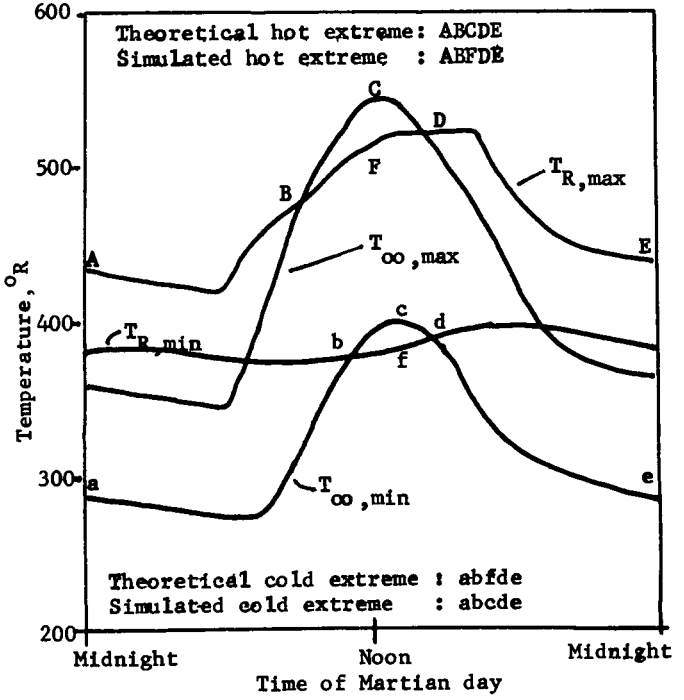

Fig. 3 – Definition of simulated thermal extremes

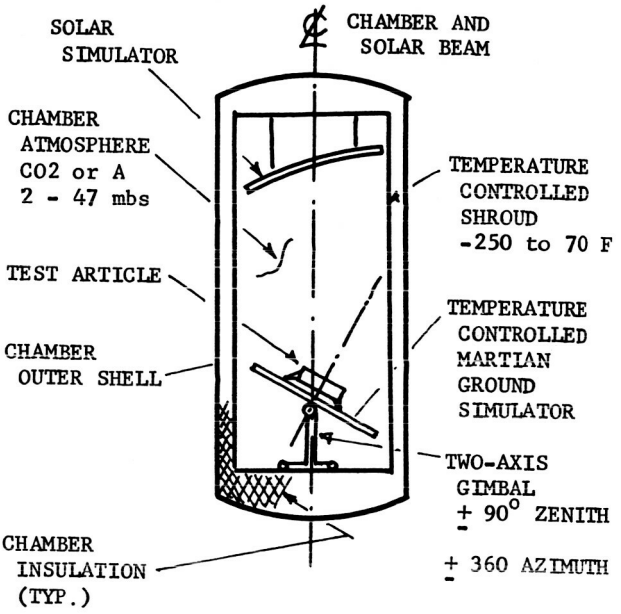

Fig. 4 – Test configuration schematic

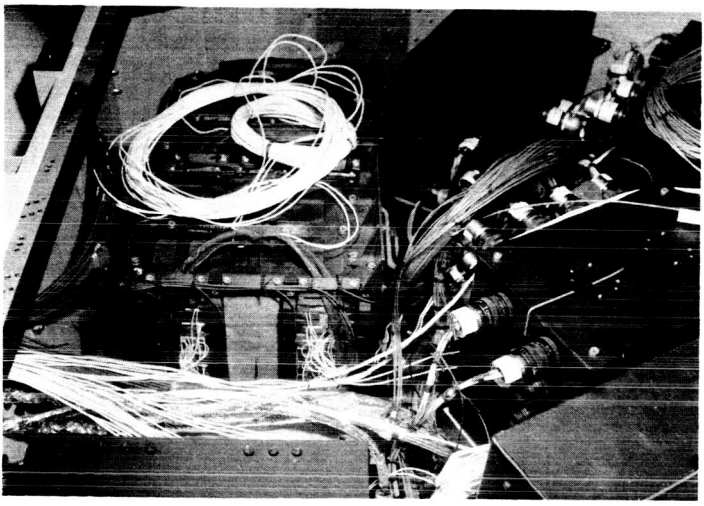

Fig. 5 – TETM thermal simulators during assembly

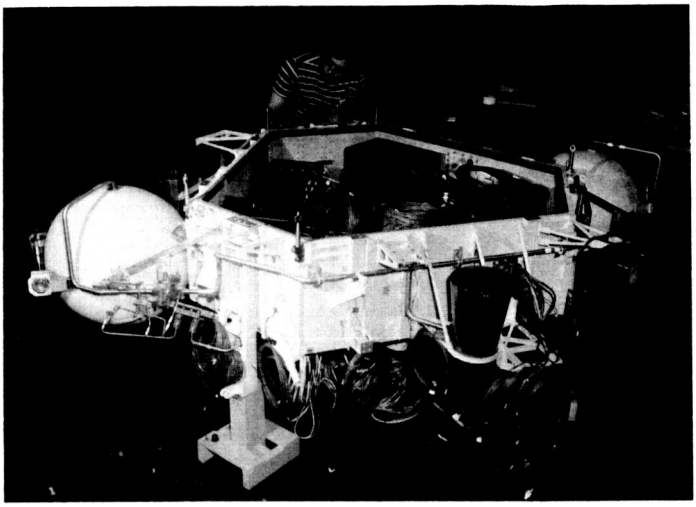

Fig. 6 – TETM during assembly - Internal equipment

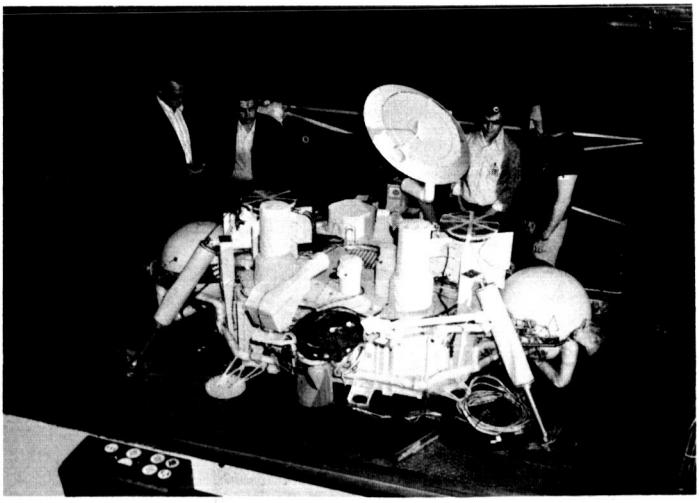

Fig. 7 – TETM during assembly - External equipment

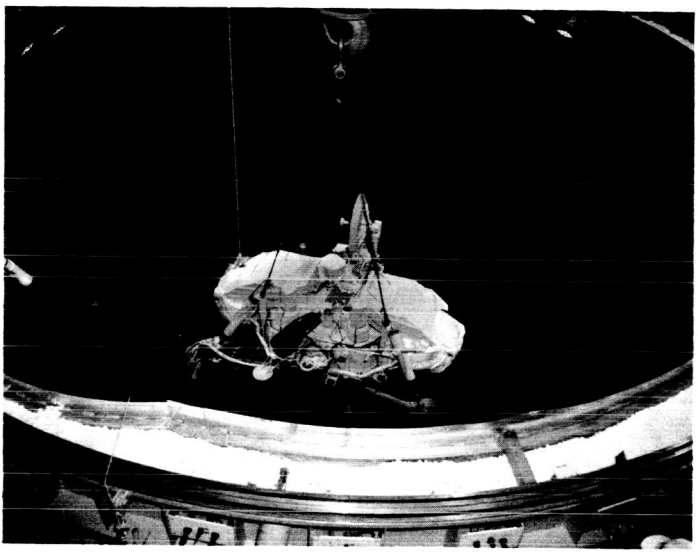

Fig. 8 – TETM being lowered into the chamber

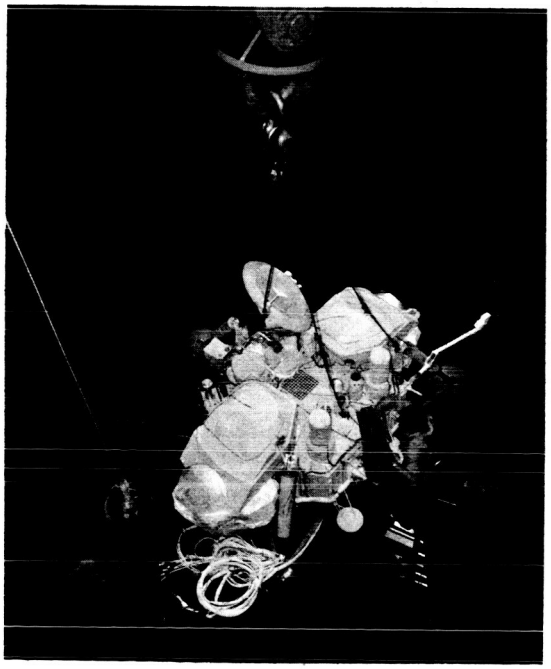

Fig. 9 – Installation and hookup inside the chamber

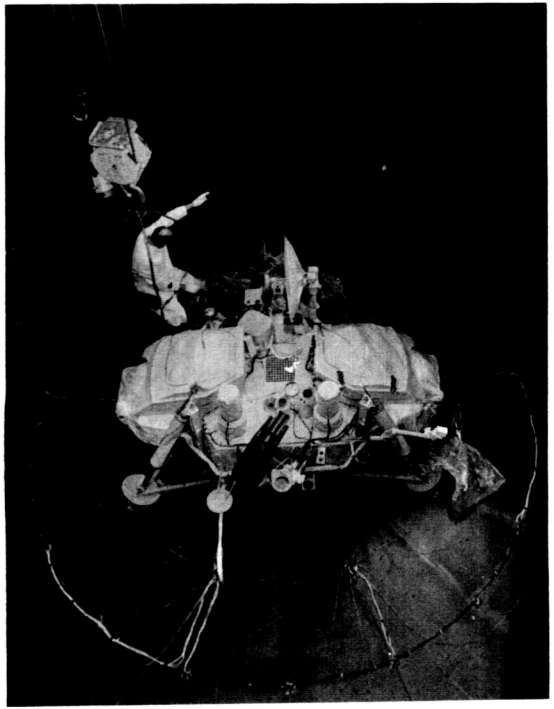

Fig. 10 – Installation complete

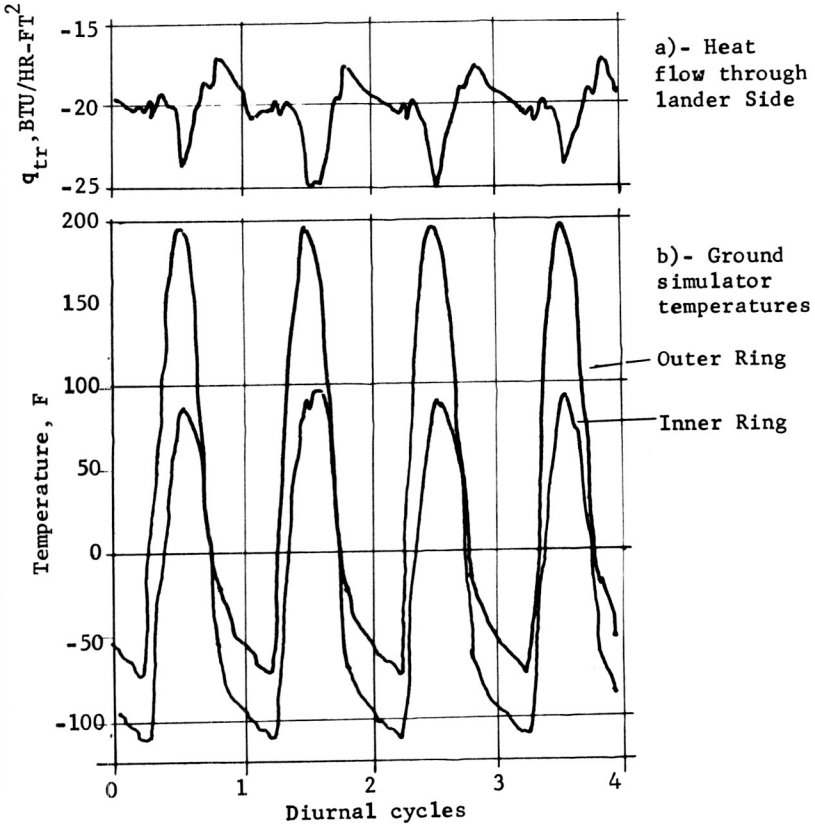

Fig. 11 – Typical data profiles - RUN NO 227

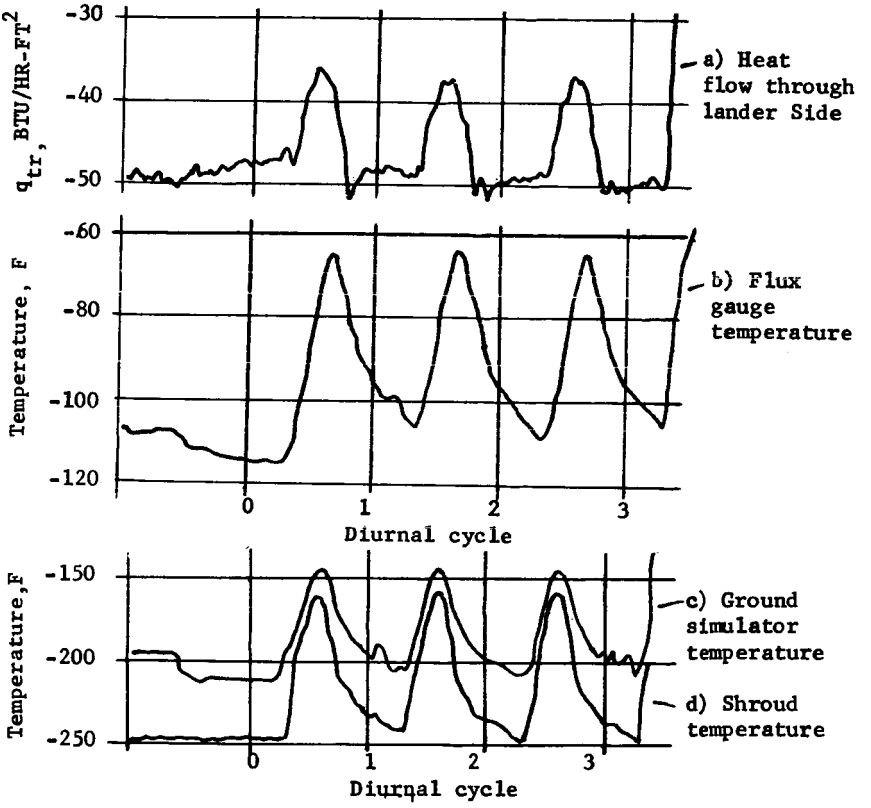

Fig. 12 – Typical data profiles - RUN NO 231

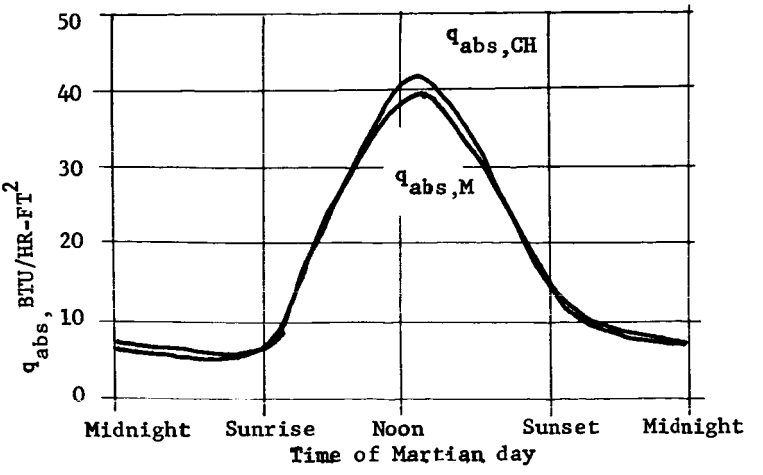

Fig. 13 – Martian vs. simulated absorbed radiation

522-137 O - 73 - 6

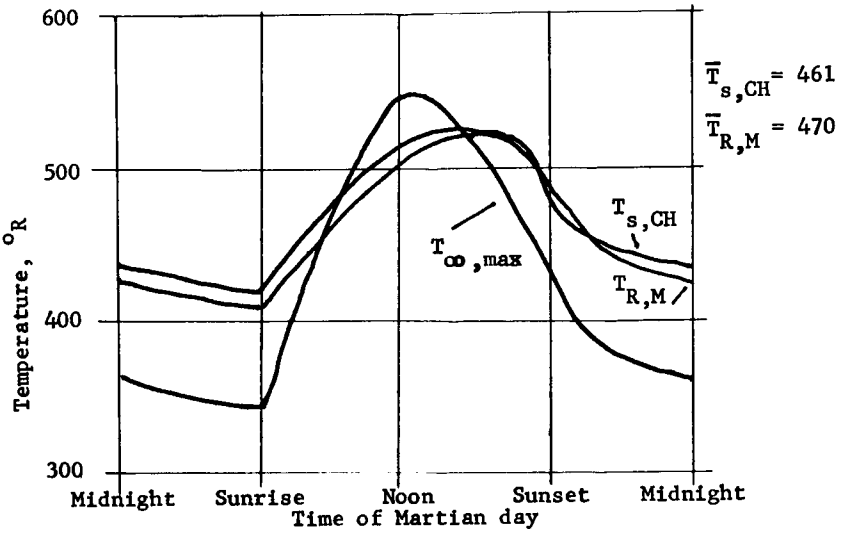

Fig. 14 — Simulated vs Martian hot extreme - Lander side - RUN NO 227

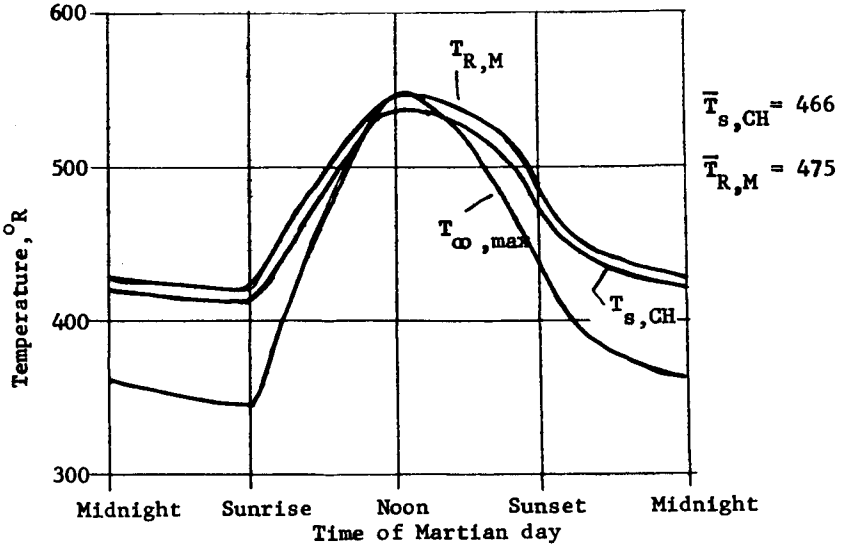

Fig. 15 — Simulated vs Martian hot extreme - Lander sides plus top - RUN NO 227

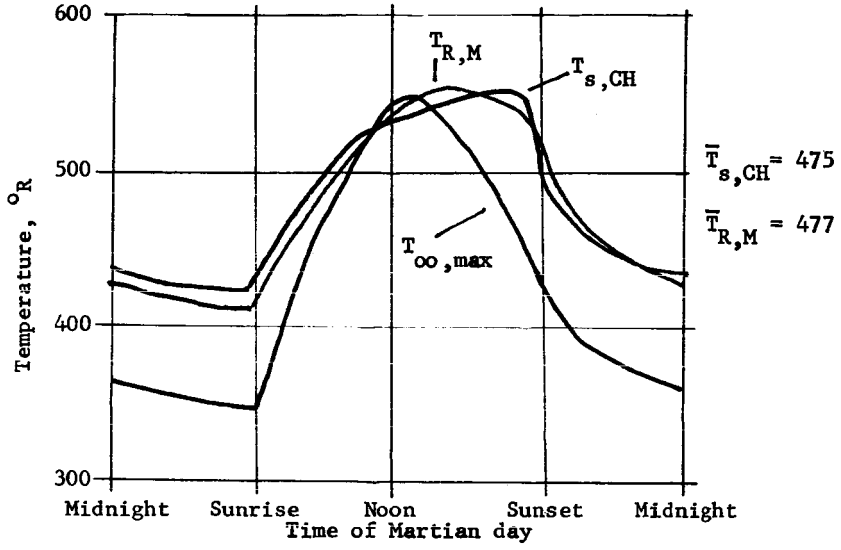

Fig. 16 – Simulated vs Martian hot extreme - Lander sides - RUN NO 223

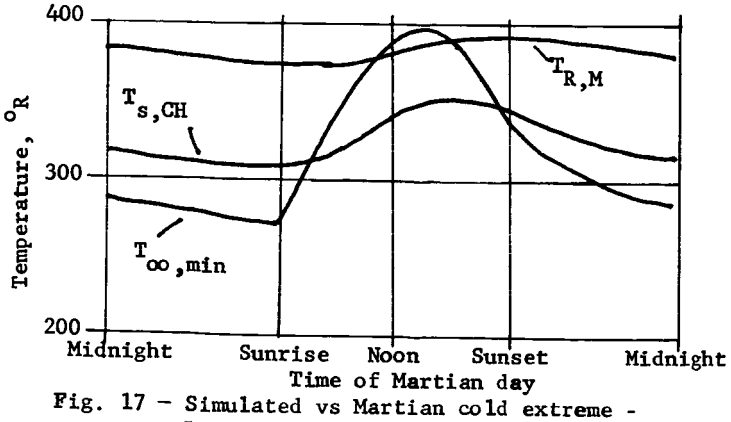

Fig. 17 – Simulated vs Martian cold extreme - Lander sides - RUN NO 231